

# Numerical analysis of masonry arch bridges: benefits and limits of damage mechanics

N. Domède and A. Sellier

*Université de Toulouse, UPS, INSA, LMDC, Toulouse, France*

**ABSTRACT:** The research presented here deals with the assessment of masonry arch bridges by means of calculation. In the University of Toulouse, a calculation tool is being developed to predict the behaviour of a masonry arch bridge under traffic loads, using an FEM code. The mechanical behaviour of the materials is modelled using a homogenised damage formulation including the effect of cracking in both tension and compression. This avoids resorting to pre-localised joint elements and, consequently, leaves a greater possibility for the failure mechanism to develop. Another benefit of this continuum approach lies in the facility allowed during meshing, since no joint elements have to be positioned in the mesh. The mechanical parameters of the blocks and of the mortar of the masonry are fitted from laboratory tests carried out on cored samples. The homogenised procedure is also numeric and is based on the same damage formulation. The whole modelling methodology is applied to an old French bridge here, and the results are discussed.

## 1 INTRODUCTION

The most recent large masonry bridges were built in the 1920's. For forty years, only modest attention was paid to masonry bridges. Studies appeared again in the late 1960's (Heymann, 1966). In France, the collapse of a bridge in 1978 (Wilson bridge at Tours) raised awareness of the need to develop an efficient calculation tool for these old bridges. Michotey and Delbecq developed a program named VOUTE, based on limit analysis theory, which was able to determine a coefficient of safety from collapse, and marketed it from 1982 to 1996 (Delbecq, 1982). Similar programs were developed at the same time in the United Kingdom (Hughes, 1997). Today, several specific software packages co-exist (Proske and Gelder, 2009). One of the most famous is RING, which analyses the collapse state only. But, despite the efforts of the UIC (Orban, 2005), no method of calculation is completely satisfactory. The research on modelling the mechanical behaviour of masonry bridges therefore continues.

In the University of Toulouse, we are developing a new calculation tool for masonry arches in order to estimate their serviceability. Our aim is not only to determine vault collapse and a safety coefficient but also to describe the mechanical response of the arches under service loads as accurately as possible in 3D. The methodology we are developing has to become a tool applicable to the largest possible number of arches with various boundary conditions (blocked or sliding support), and in three dimensions, in order to be able to take account of transversal damage mechanisms not considered in the earlier model..

We have chosen to describe the mechanical behaviour of the constitutive masonries using a damage model. This model presents the following advantages:

Firstly, the location of cracks is not a hypothesis as in joint element or discrete element calculations since the cracks and damage zones are the natural consequences of the localization process induced by the softening phase of the behaviour law.

Secondly, the damage model considers unilateral aspects of the behaviour law; in masonry they are due to the possibility of crack reclosing and the crushing of the material in compression.

The portability of the model is not a problem since a damage model can be implemented in any finite element code.

Lastly, the damage model allows the fracture energy to be managed not only in tension but also in compression.

In the first section below, we describe the damage model developed in Toulouse and its application to masonry material. Then, a case study of a French bridge and its results are presented.

## DAMAGE MODEL

The damage model used here is an orthotropic based one. It is a variant of the initial model described in detail by Sellier and Bary. The following presentation adopts the six-dimensional vectorial representation of the classical  $3 \times 3$  symmetric tensors. An effective stress  $\underline{\underline{\sigma}}^e$  is computed according to the elastic strain  $\underline{\underline{\varepsilon}}^e$ , using the sound material stiffness matrix  $\underline{\underline{C}}^0$ :

$$\underline{\underline{\sigma}}^e = \underline{\underline{C}}^0 \cdot \underline{\underline{\varepsilon}}^e \quad (1)$$

The effective stresses are divided into tension,  $\underline{\underline{\sigma}}^t$ , and compression,  $\underline{\underline{\sigma}}^c$ , parts according to the sign of the main stresses. The positive part is used in a Rankine Criterion (Maximal Tensile Stress criterion, also called MTS by Erdogan and Sih, (1963). This criterion is used to assess the tensile damage tensor  $\underline{\underline{D}}^t$  which affects the positive effective stresses. The negative part of the effective stresses is used to assess a Drucker Prager equivalent stress defined by:

$$\tilde{\sigma}^{DP} = \sqrt{\frac{J^{2d}}{6}} + \delta \frac{I^t}{3} \quad (2)$$

With  $J^{2d}$  the second invariant of the deviator of  $\underline{\underline{\sigma}}^e$ ,  $I^t$  the trace of  $\underline{\underline{\sigma}}^e$  and  $\delta$  the Drucker Prager constant, which depends on the internal friction angle  $\varphi$  as follows in Eq.3.

$$\delta = \frac{2\sqrt{3} \sin \varphi}{3 - \sin \varphi} \quad (3)$$

The Drucker Prager equivalent stress is used to assess a compressive damage tensor. In Eq 4, both the tensile and compressive damage affects the effective stresses orthotropically to give the stress to be used at integration points of the finite element code. The internal variables that characterize the damage state are noted  $D^t$  in the tensile domain and  $D^c$  in compressive domain.

$$\underline{\underline{\sigma}} = (\underline{\underline{I}} - \underline{\underline{D}}^c) \cdot ((\underline{\underline{I}} - \underline{\underline{D}}^t) \cdot \underline{\underline{\sigma}}^t + \underline{\underline{\sigma}}^c) \quad (4)$$

with  $\underline{\underline{I}}$  the identity tensor.

The evolution laws used to link the criteria and the damage lead to a softening phase of the behaviour laws as illustrated in Fig.1. To avoid a dependence of the finite element solution on the mesh size (due to the localization induced by softening), the damage also depends on the finite element size. The model also allows a variable to be plotted that is interesting for practitioners: the Crack Mouth Opening Displacement (CMOD). It can be plotted directly at the Gauss point during the finite element solving procedure or post-treated at the end of the whole calculation for each substep. This CMOD depends not only on the damage state but also on the strain state. In the present modelling, it corresponds to the averaged crack opening displacement computed assuming a single localised crack in the element. It is approached in the main direction of the Rankine effective stress by the following expression:

$$CMOD_m = l_m \left( \underline{\underline{\varepsilon}}^e \cdot \underline{\underline{\varepsilon}}_m \right) \left( \frac{D_m^t - D_{peak}^t}{1 - D_{peak}^t} \right) H(\sigma_m^R - E \varepsilon_{peak}^t) H\left( \frac{D_m^t - D_{peak}^t}{1 - D_{peak}^t} \right) \quad (5)$$

With :

$l_m$  : finite element length in the direction  $\underline{\underline{\varepsilon}}_m$  ;

$\underline{\underline{\varepsilon}}_m$  : vectorial representation of the elementary matrix obtained by the tensorial product of the unitary vector in the main direction 'm' ;

- $D_m^t$  : tensile damage value in the corresponding main direction ‘m’;
- $D_{peak}^t$  : damage value at the peak of the behaviour law in tension (point 1 in Fig.1);
- $\sigma_m^R$  : current value of the Rankine criterion in the direction ‘m’;
- $E\varepsilon_{peak}^t$  : the equivalent stress reached in direct tension for the point 1 in Fig.1;
- $H(X) = 1$  for  $X > 0$ , 0 otherwise: Heaviside function.

An illustration of the benefit of using this variable instead of the classic damage variable is given at the end of this paper. The advantage is that, even if much limited cracking occurs in a massive structure, only the main cracks will stay open until failure occurs, and all the other surrounding ones will be reclosed. CMOD is then able to capture this main crack among the multiple damaged elements.

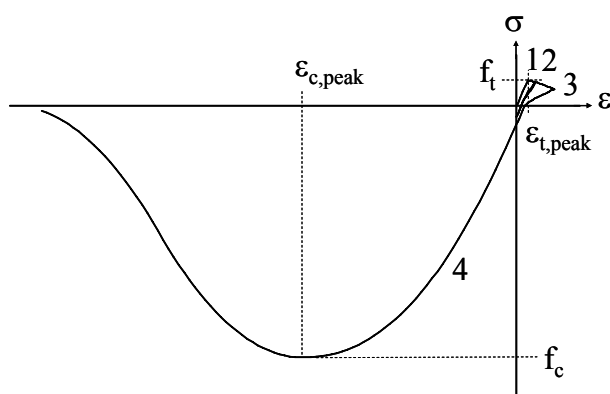


Figure 1 : damage model, behaviour under cyclic axial load (cycle order numbered 1 to 4).

CASE STUDY

The masonry arch presented here has already been studied with an elasto-plastic finite element model for compressive behaviour coupled with joint elements to describe tensile cracking (Domède, 2006). Our aim is now to build a comparative study and identify the advantages and disadvantages of the damage model.

The bridge is a circular, single span built in 1870, with length  $L=14.37m$ , radius  $R = 10.75m$ , width = 4.80 m and keystone 79 cm thick (see Fig.2 and Fig.3). It is composed of four different masonries. The vault is in brick, the lateral strings and springing in cut stone, the spandrel walls in stone arranged in opus incertum, and the fill in rubble. The mortar is a hydraulic lime mortar without cement. Fig.2 shows the different parts of the bridge with the mesh used for the finite element analysis. Fig.3 gives some photos of details taken in the field.

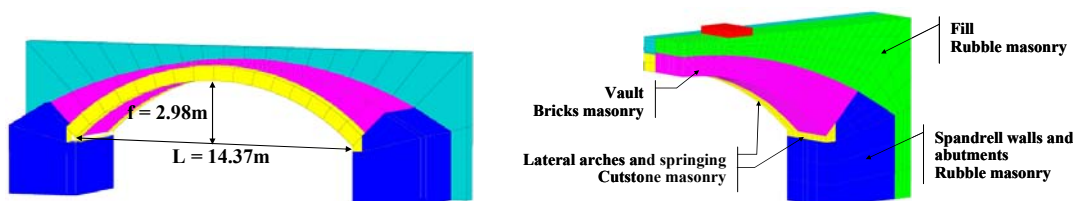


Figure 2 : geometry of the arch bridge studied.

View without the front spandrel wall and the fill (left), location of the 4 masonries (right).



Figure 3 : images of the bridges.

### Modelling of materials

To determine the homogenized model of each of the 4 different masonries, we applied a numerical method validated by an experimental approach on brick masonry. The steps were the following:

- (1) Experimental individual characterization of the mortar and of the bricks (compressive tests),
- (2) Fitting of the mortar and the brick individual behaviour laws with a damage model,
- (3) Tests of multilayer brick – mortar samples in order to determine the confinement effect on the mortar, and the cracking scheme (Fig.4),
- (4) Modelling of the multilayer sample and parametric study,
- (5) Fitting of a single damage parameter set on last results for the homogenised masonry behaviour law.

The mechanical characteristics in compression, the compressive strength  $f_c$ , the strain at peak  $\epsilon_{c,peak}$ , the fracture energy in compression  $G_c$ , the Young modulus  $E$  and the Poisson coefficient  $\nu$ , chosen for the 4 masonries of the bridge studied are given in Tab. 1. The shear angle  $\varphi$  equals  $20^\circ$  ( $\delta = 0.45$ ). The stress-strain curves are given in Fig.5.

In tension, the same damage law, corresponding to the approximated weakest zone, i.e. the brick mortar interfaces, is adopted for all the masonries, with the following characteristics: tensile strength  $f_t = 0.1\text{MPa}$ , strain at peak  $\epsilon_{t,peak} = f_t / E$ , fracture energy in tension  $G_t = 0.002\text{N/mm}$ .

Table 1 : mechanical characteristics of blocks and masonries in compression

		$f_c$ N/mm <sup>2</sup>	$\epsilon_{c,peak}$ mm/m	$G_c$ N/mm	$E$ N/mm <sup>2</sup>	$\nu$
Brick masonry	Vault	11.9	3.5	50.	6800	0.15
Natural stone	Stone string	49.5	3.5	100.	28100	0.25
masonries	Spandrel wall	42.5	3.5	200.	21700	0.2
	Fill	42.5	3.5	200.	21700	0.2

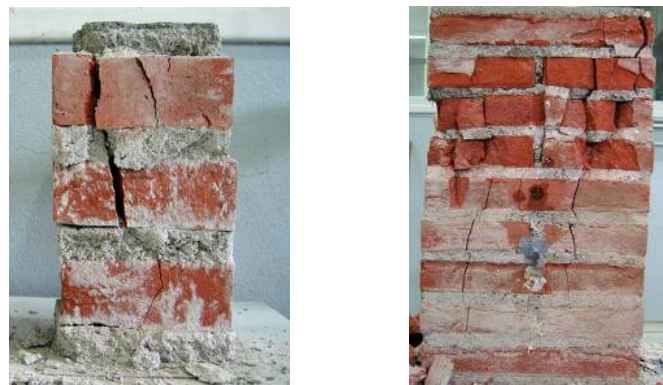


Figure 4 : images of multilayer and wall samples after tests.

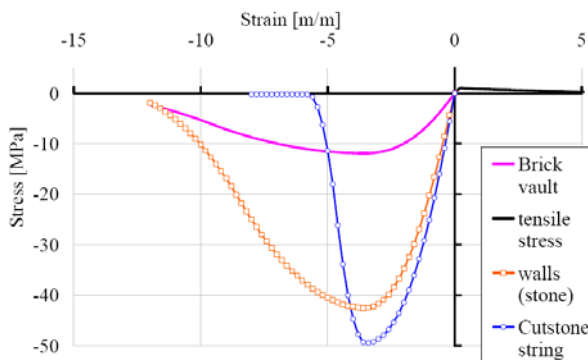


Figure 5 : homogeneous damage model of the 4 masonries.

*Bridge modelling*

The mesh of the bridge (Fig.2) has been automated but requires a few parameters to be given by the user (position of the centre of the circle describing the intrados, its radius and its open angle, level of the abutments, highest level of the spandrel walls, thickness at crown, dimensions of the abutments, thickness of the spandrel walls). Each of the 4 different masonries is described by a damage model presented above. The mesh of the masonry is made with 3D massive cubic finite elements without any element interfaces. In this study, the bridge cannot slip on the ground, but this boundary condition could be easily modified.

The bridge is straight and has axial symmetry. In order to decrease the calculation time, only half of the bridge is modelled (half the width).

*Loading of the bridge*

The bridge is first loaded by its own weight (10 MN) and next by an off-centre vehicle weight located at a third of the span (arrows in Fig.6). The vehicle is represented by two axles, with geometry in conformity with type TS of Eurocode 1. The two corresponding localized loads are applied to intermediate elastic solid (in red on Fig.6) added to diffuse localized load effects and limit punching in the fill. The transverse positioning of this tandem is central (half of the axles are positioned on half of the bridge). The load is increased until the bridge collapses.

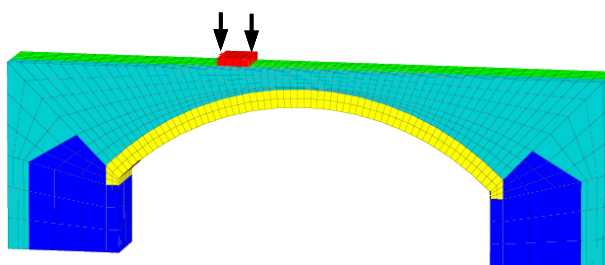


Figure 6 : location of the loads. View of half of the bridge mesh from outside

**RESULTS**

The results are commented in terms of displacements, limit load, damage variables and location of opened cracks. They are compared with the results obtained 3 years ago using the plastic model associated with joint elements (Domède, 2006). To facilitate comparison, the essential results of the first calculation are briefly recalled.

### Reminder of main results obtained with the previous models

Masonry behaviour in compression was modelled with plastic Von Mises materials in massive finite elements. The cracking was possible through joint elements with a Coulomb model. They were positioned a priori only transversally (see Fig.7). In a first calculation, the abutments were able to slide on the ground because of the positioning of the joint elements. The collapse load was then around 7MN.

If the abutments were blocked on the ground, the bridge bearing capacity increased until the compression strength of one of the masonry elements was reached. But it was also noticed that the compressive stress gradient between the stone string and the brick vault created shear stresses in the interface between these two zones, concomitant with transverse tensile stresses. The risk of localized longitudinal failure was clear from 4MN but, without longitudinal joint elements in the model, it was not possible to demonstrate this phenomenon.

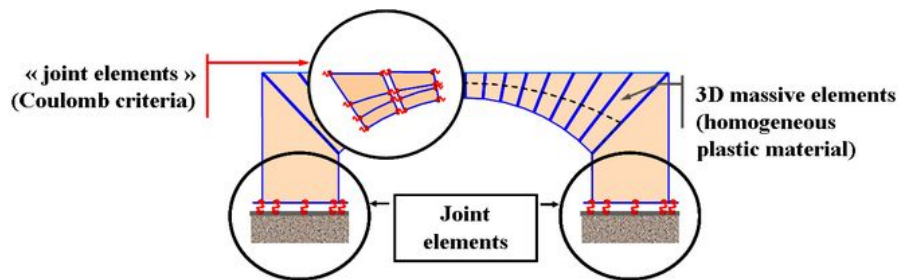


Figure 7 : model with joint elements used three years ago

### Results obtained with the proposed damage model

With the proposed damage model, the maximum load reached was 4.3MN. Beyond this threshold, the deformation of the bridge was uncontrolled (Fig.8).

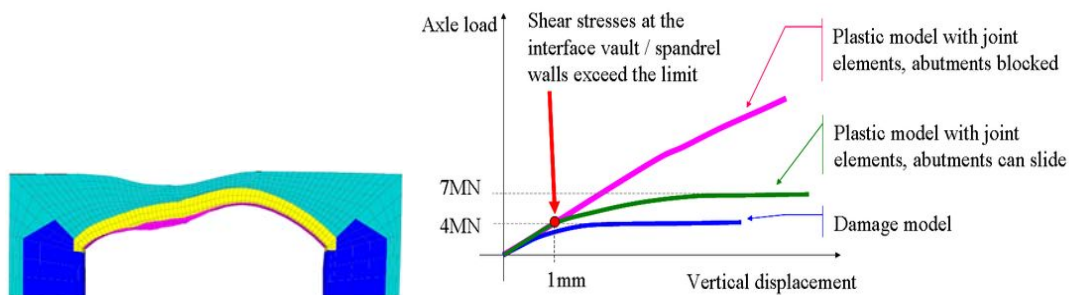


Figure 8 : view of the deflected bridge and load – displacement curve. Comparison between plastic model with joint elements and damage model.

Even though the failure load has the same order of magnitude as in the previous model (with joint and without damage), the failure mode forks at this value and becomes very different beyond the corresponding displacement, as explained in the following paragraph.

### Damage and Crack opening

An idealized view of the cracking pattern obtained with the damage model is shown in fig. 10. It corresponds to the last step described in Fig. 11. The two first cracks are transverse but, finally, the most widely opened cracks are longitudinal. They are located along the cut stone lateral string. This failure mechanism could not be captured by the previous joint element model because of the impossibility crossing the elements.

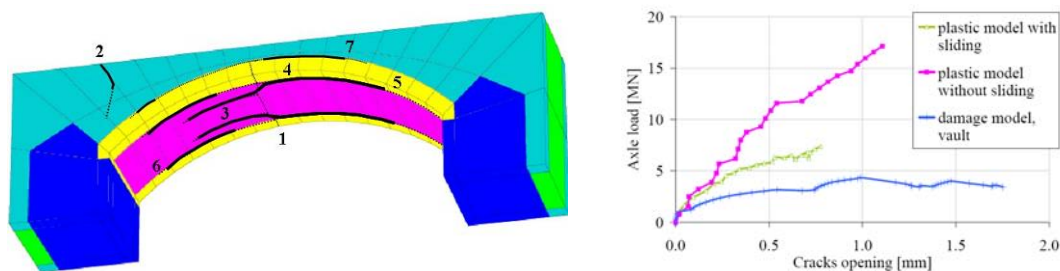


Figure 10 : Cracking state with order of appearance of cracks (left), load – crack opening curve (right)

Fig.11 gives the increase of tensile damage ( $D_t$ ) and crack opening displacement (CMOD), step by step.  $D_c$  is not shown because no element was damaged in compression. Comparing CMOD and  $D_t$  in Fig.11 shows that, although the damage seems to be relatively generalised at the end of the calculation, only a few elements present a significant CMOD. This means that most of the cracking initiated does not propagate, because of the localisation phenomena controlled by the softening part of the damage model.

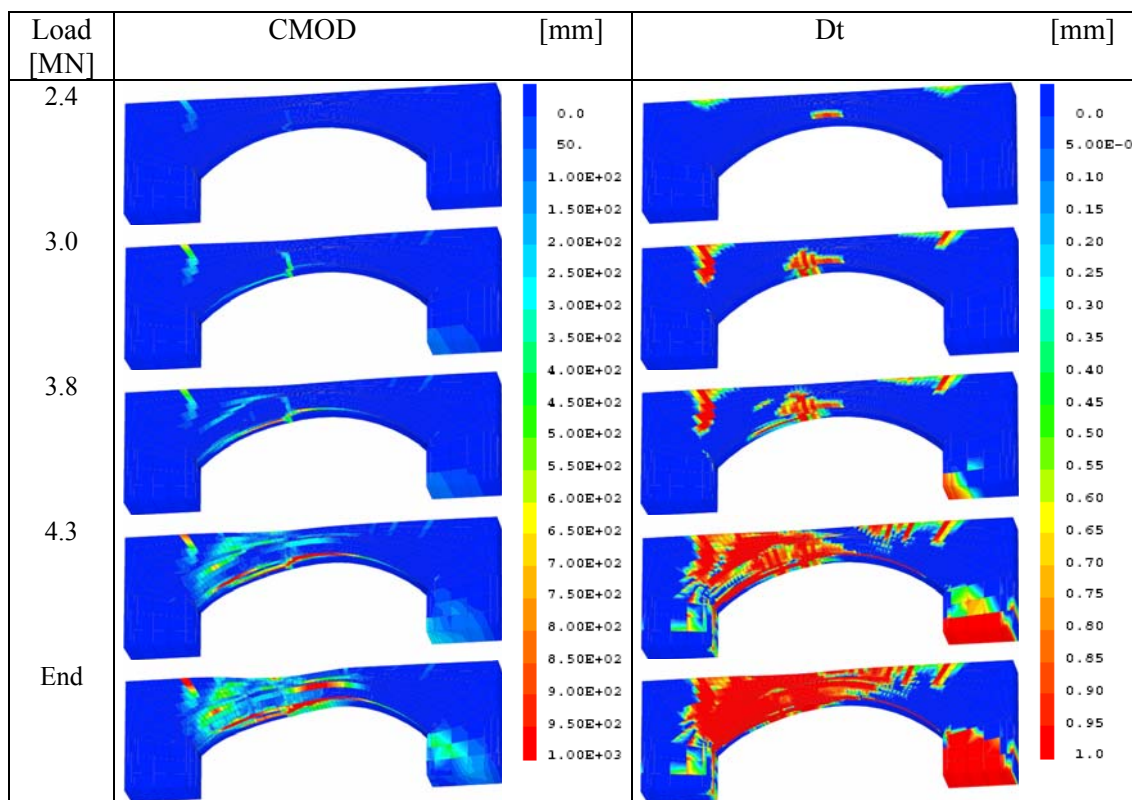


Figure 11 : Increase of CMOD and  $D_t$  with the axle loads. View of half the bridge.

### CONCLUSION AND PROSPECTS

In this paper, the calculation of a masonry arch bridge under loads with a damage model in 3D has been presented. Unlike the joint element model, it allows automatic determination of the crack locations, whatever the underlying mechanical phenomenon (tension, compression or shear). The width of the cracks is calculated step by step, which allows a serviceability limit state to be chosen in terms of crack opening limit. By studying the load – deflection curves, it is possible to define an ultimate limit state.

This model is currently being improved in association with the SNCF, the French railway corporation, in order to create a finite element toolbox usable by practitioners in charge of the maintenance and restoration of the masonry bridges.

## REFERENCES

- Chairmoon K. and Attard M., 2008. Experimental and numerical investigation of masonry under three-point bending (in-plane), *Eng Structures*, p.31, p.103-112.
- Delbecq J.M., Service d'Etudes Techniques des Routes et Autoroutes. Les ponts en maçonnerie, historique, stabilité, utilisation du programme VOUTE, 1982.
- Domède, N., 2006. Méthode de requalification des ponts en maçonnerie, Ph D. thesis, INSA de Toulouse, France.
- Domède N. and Sellier A., 2010. Experimental and numerical analysis of behaviour of old brick masonries, SAHC conference, October 2010.
- Erdogan F. and Sih G.C., 1963. On the crack extension in plates under plane loading and transverse shear, *Journal of Basic Engineering*, p.85, p.519-527.
- Fernandes FM., Lourenço PB. and Castro F., 2010. Materials, technologies and practice in historic heritage structures, Springer Netherlands, DOI 10.1007/978-90-481-2684-2
- Heymann J., 1966. The stone skeleton, *Int, Journal of Solids and Structures*, vol. 2.
- Hughes TG. and Blackler MJ., 1995. A review of the UK masonry assessment methods, *Proc Inst Civil Eng* 110:373-382.
- Lourenço P-B., 1996. Computational strategies for masonry structures, Ph D. thesis, Delft, Netherlands.
- Luciano R. and Sacco E., 1998. A damage model for masonry structures, *European Journal of Mechanics A-solids*, p.17, p.285-303.
- Pietruszczak S. and Ushaksaraei R., 2003. Description of inelastic behaviour of structural masonry, *International Journal of Solids and Structures*, p.40, p.4003-4019.
- Proske D. and Van Gerlder P., 2009. Safety of Historical Stone Arch Bridges, Springer DOI 10.0007/978-3-540-77618-5.
- Orban Z. and UIC., 2005. Improving assessment optimisation of maintenance and development of database for masonry arch bridges, progress report.
- Reyes E., Casati M J. and Galvez J C., 2008. Cohesive crack model for mixed mode fracture of brick masonry, *Int J Fracture*, p.151, p.29-55.
- RING, 2003, The University of Sheffield, [www.shef.ac.uk/ring](http://www.shef.ac.uk/ring).
- Sellier A. and Bary B., 2002. Coupled damage tensors and weakest link theory for describing crack induced orthotropy in concrete, *Engineering Fracture Mechanics* n°16